15

Process in multimode fiber optical vortices and the study Features of the interference of their excitation

© A.A. Makovetskii, A.A. Zamyatin

Fryazino Branch, Kotel'nikov Institute of Radio Engineering and Electronics, Russian Academy of Sciences, Fryazino, Moscow oblast, Russia

e-mail: maz226@ms.ire.rssi.ru

Received December 16, 2022
Revised May 10, 2023
Accepted May 10, 2023

Experiments on excitation of meridional rays and optical vortices in short silica-polymer optical fibers were carried out using a laser ($\lambda = 532$ nm) and lenses with different numerical aperture values. For research, we have drawn out samples of optical fibers with a core diameter of $200-800\,\mu$ microns and a reflective shell made of various polymers. In experiments, under different excitation conditions, radiation intensity distributions were recorded at the output end of the optical fiber (in the near field) and in the far field. Caustic control allowed to excite different groups of optical vortices in and observe various topologies of intermode interference, including spiral structures. A qualitative analysis of the experimental results was carried out.

Keywords: multimode optical fiber, radiation intensity distributions in near and far fields, optical vortices, caustics, intermode interference.

DOI: 10.61011/EOS.2023.08.57291.4454-23

Introduction

Optical beams with wavefront rotation, called optical vortices, are widely used in scientific research and technology due to their specific properties [1,2]. Optical vortices are formed in free space when a laser beam passes through turbulent areas of the atmosphere. They are also excited in optical fibers (OF) [3]. In multimode OFs, they can arise as a result of the transformation of groups of hybrid modes in randomly occurring sections of the fiber with birefringence [4]. A characteristic feature of an OF optical vortex (as well as that of a hybrid mode) is a dark spot in the center of the radiation intensity distribution at the output end of the OF and a ring pattern of the radiation in the far field. Hybrid modes in an OF are excited by an oblique focused laser beam, which is offset relative to the center of the OF input end and does not cross the OF axis [5,6]. The classic method for detecting an optical vortex is its interference with a plane wave, the pattern of which is a multi-turn spiral [7,8].

The most detailed studies of the excitation of hybrid modes and optical vortices in short sections of multimode OFs with a fiber core diameter from 100 to $800\,\mu$m were carried out in [5,9,10]. In these studies, the OFs were excited by a laser beam, both directly and with a focused lens (from MIKMED-V-1-20 microscope). The radiation intensity distributions at the OF end and in the far field (at distances of up to 1 mm from the end) were recorded with a digital camera. At certain settings, spiral interference patterns were observed in the far field, and a quasi-beam interpretation of their occurrence was given. However, the measurement scheme did not allowed recording the radiation emitted from the OF at distances of 50−300 mm from its end, which are suitable for direct visual analysis of the image. In addition, the effect of parameters of the lens used on the efficiency of optical vortices excitation, the issues of radiation caustics in OFs and its effect on the distribution of radiation intensity in the far field have not been studied.

In this context, the purpose of the study was as follows:

1) conducting experiments on the excitation of hybrid modes (oblique beams) and optical vortices in short (0.1−0.5 m) multimode silica-polymer OFs with a core diameter of $200-800\,\mu$m under various excitation conditions with the use of lenses with different numerical aperture values;

2) qualitative analysis of the patterns of excited fields in the near-field (at the output end of the OF) and far-field diffraction regions in order to identify the effects of intermode interference.

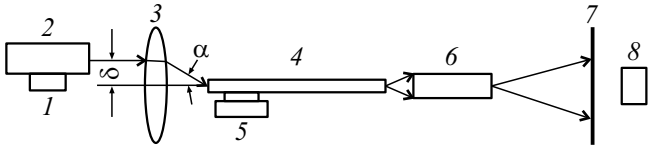

Figure 1. Diagrams for introducing radiation into the OF and recording radiation intensity distributions in the near-field and far-field regions (view in the horizontal plane): *1* — table for shifting the laser axis relative to the lens axis in the horizontal plane, *2* — LG 303 laser ($\lambda = 532$ nm), *3* — lens, *4* — OF under study, *5* — adjustment unit with 3-coordinate linear feed and 2-coordinate angular adjustment of the OF input end, *6* — microscope, *7* — paper screen, *8* — digital camera.

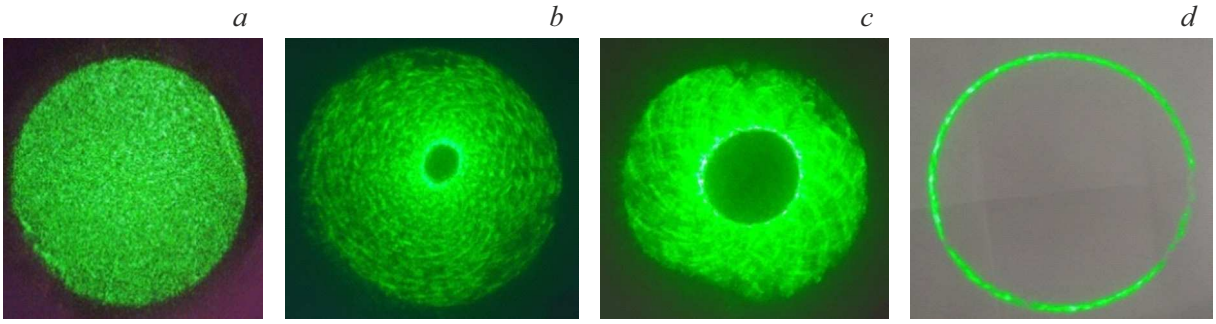

Figure 2. Radiation field intensity distributions ($\lambda = 532\,\text{nm}$) in SP-SIEL/600 μm with a length of $l = 17\,\text{cm}$ in the near-field region (at the end of the OF); lens $10^{\times}$, 0.4. Photo (a) — speckle pattern, $\delta = 0\,\text{mm}$. Photo (b, c, d) — patterns with caustics, $\delta = 3.5\,\text{mm}$; the magnitude of x_s consistently increases from $\approx 10\,\mu\text{m}$ (b) to $\approx 280\,\mu\text{m}$ (d).

Methods

The diagram of the experimental setup for exciting optical vortices in OF and recording their radiation intensities in the near-field and far-field regions is shown in Fig. 1.

Radiation of laser *2* (LGLaser 303, $\lambda = 532\,\text{nm}$) was introduced into OF *4* through lens *3* initially aligned coaxially with the fiber. Lenses used were LOMO $10^{\times}$, 0.4; F-6.16A-0.65; F-$2.8^{\times}$, 1.25, differing in the values of numerical aperture and focal length. Adjustment table *1* implemented an adjustable transverse shift δ of the laser axis relative to the lens axis in the horizontal plane. At $\delta = 0$, the focused beam was incident to the center of the OF end at an angle of $\alpha = 0$ to the OF axis, exciting low-aperture meridional beams. The introduction of a shift $\delta > 0$ resulted in an oblique incidence of the beam to the OF end ($\alpha > 0$) and the excitation of meridional beams with a larger radiation aperture. The table shows measured values of the of the focused beam diameter d_n, its divergence $\delta\varphi$, as well as the maximum angle of incidence of the beam α_m for the three lenses used. The dependence of the angle of incidence α on the shift δ was determined by the following formula: $\alpha(\delta) \approx \alpha_m \delta/\delta_m$, where δ_m being the maximum shift allowed for a given lens.

To excite optical vortices, the point of incidence of the beam on the input OF end was shifted from its center in the vertical direction by a certain amount of $x_s \in (0, \frac{D}{2} - D/2)$, where D is the OF core diameter. This was carried out using mechanical adjustment unit *6*, where the input OF end was fixed. The adjustment unit had a 2-coordinate angular adjustment in the horizontal and vertical planes and a 3-coordinate linear feed in x, y, z directions. However, the determining adjustment of the unit is the linear feed in the vertical direction (the y-feed). Linear feeds in x-direction and z-direction, as well as angular adjustments γ and δ were used for fine tuning.

To record the field in the near-field region, microscope *5* was adjusted to the output OF end. In this case, the beams emitted from the OF formed an enlarged image of the end on paper screen *7*, which was recorded by a digital camera. The distance from the microscope eyepiece to the screen was 30−50 cm.

When recording the field in the far-field region, the microscope was removed from the set-up. The image was taken from a screen located at a distance of 5−20 cm.

For experiments, we fabricated samples of silica-polymer (SP) optical fibers with fiber core diameters of $D = 200$, 400 μm, 600 μm, and 800 μm with a reflective shell made of SIEL-159 -305 silicon-organic elastomer. Also, OFs with a core diameter of 400 μm with shells made of crystallizing copolymer of tetrafluoroethylene with Tefzel ethylene were fabricated and tested. The nominal numerical aperture of the studied OFs was 0.4−0.45. In the following text, we will denote OFs as follows: SP-grade of shell/core diameter.

Results. Discussion

Control of radiation caustics in OFs

By adjusting the δ and x_s parameters of the optical geometry, various groups of meridional and hybrid modes can be excited in OFs. Typical photos of radiation intensity distributions at the output end of SP-SIEL/600 μm with a length of $l = 17\,\text{cm}$ are shown in Fig. 2.

With $\delta < 2\,\text{mm}$ and $x_s \approx 0\,\mu\text{m}$, spotted speckle patterns were formed at the OF end (Fig. 2, a), which are typical for meridional beams. With $6\,\text{mm} > \delta > 2\,\text{mm}$ and $x_s > 0\,\mu\text{m}$, field patterns with caustics were formed (with a dark spot in the center of the OF end, Fig. 2 , b , c, d). Patterns like these are typical for hybrid modes and optical vortices. We define the caustic-characterizing quantity as $\chi = d/D$, where d being internal diameter of the dark spot at the OF end, D being diameter of the OF core. The value of χ was determined mainly by the xs value and weakly depended on the axial shift δ. All three photos with caustics were taken with the same $\delta = 3.5\,\text{mm}$ but with different values of x_s. It can be seen from them that when x_s changed from 10 to 280 μm, the χ increased from ≈ 0.15 to ≈ 0.9. From the point of view of wave analysis, χ is determined by the smallest value of the azimuthal number $m_{\min}$ for a group of excited optical vortices: $m_{\min} < m_{\max}$, where

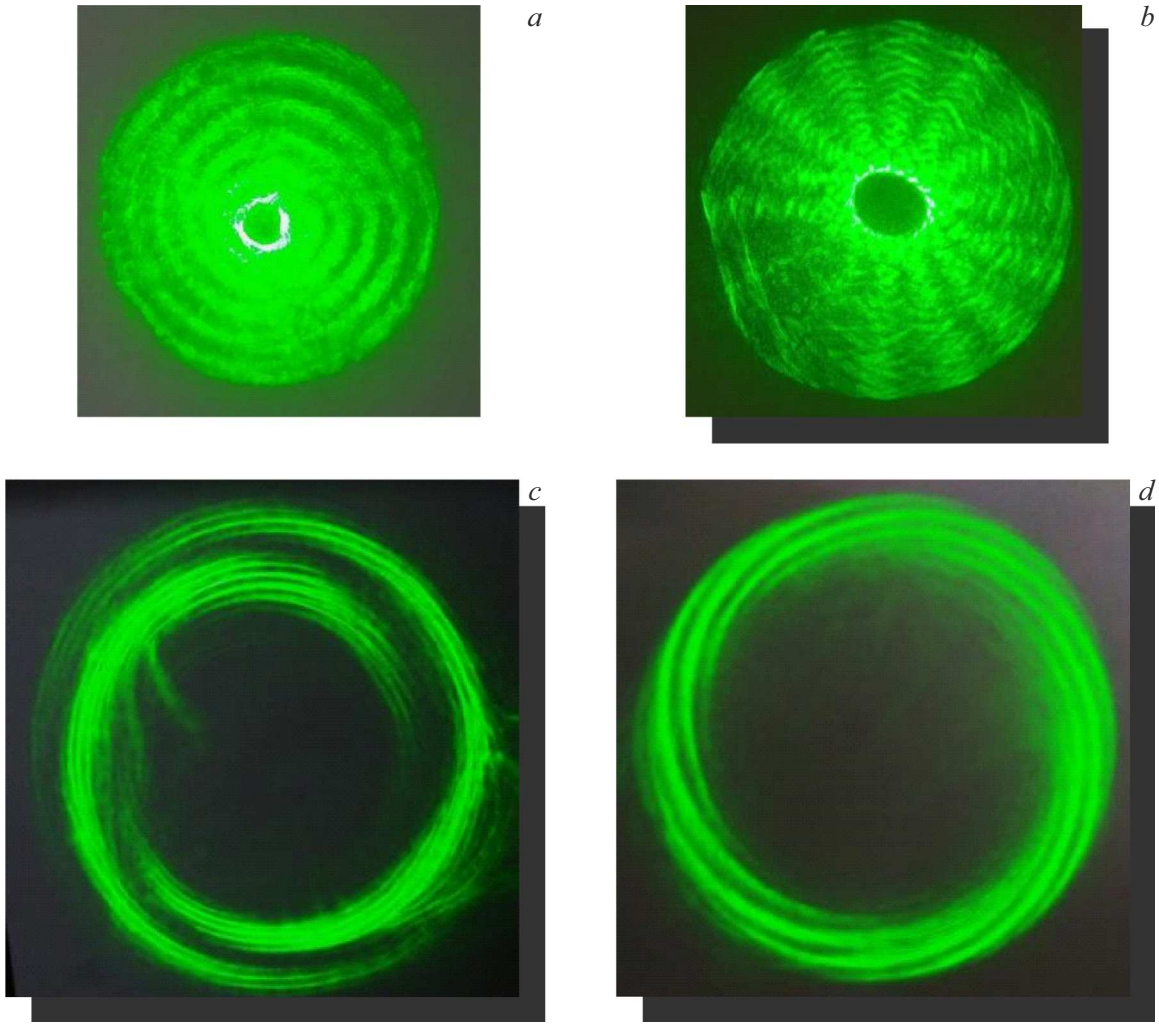

Figure 3. Radiation field intensity distributions ($\lambda = 532$ nm) for SP-SIEL/600 μm with a length of $l = 17$ cm in the near-field (a, b) and far-field (c, d) regions; lens F 6.16-0.65. Photos (a, c) were taken with $\delta \approx 1$ mm, $x_s \approx 10\,\mu$m, $\chi \approx 0.12$; photos (b, d) were taken with $\delta \approx 2$ mm, $x_s \approx 20\,\mu$m, $\chi \approx 0.22$.

$m_{\max}$ is maximum (for a given OF) value of the azimuthal number. $m_{\max}$ of SP-SIEL/200 μm, SP-SIEL/400 μm, and SP-SIEL/600 μm optical fibers can be estimated as 476, 943 and 1430, respectively [11]. The increased radiation brightness at the inner boundary of the caustic, which is noticeable in the photo, is indicative of the predominant excitation of a group of hybrid modes with azimuthal numbers close to $m_{\min}$.

Interference patterns formed by SP-SIEL/600 (200, 400, 800) μm when using a F 6.16-0.6 lens

The most diverse interference patterns in the far-field region were obtained with short sections of SP-SIEL/600 μm using a F 6.16-0.65 lens. Numerical aperture for this lens (0.65) is larger than the nominal numerical apertures of the studied OFs (0.4–0.45). Examples of recorded interference patterns for short OFs of various lengths are shown in Fig. 3–5. Qualitatively, their topologies are as follows: 1) a bifilar spiral with each branch consisting of several thinner fragments of spirals (Fig. 3, c); 2) a multifilar spiral (Fig. 3, d); 3) a ring-envelope consisting of a set of nested arc segments (Fig. 4, b, c); 4) a ring-envelope with spotting noticeable inside instead of arc segments (Fig. 5, b).

It should be noted that the bifilar spiral corresponds to a ring pattern of the field at the OF end, and the multifilar spiral corresponds to a radial pattern. At the same time, it is possible to excite spirals twisted both clockwise and counterclockwise.

Spiral patterns and ring-envelopes appeared with visually contrasting caustics. Such a caustic is a thin ring-shaped area with bright points located azimuthally in it (Fig. 3, a, b; Fig. 4, a). When the spirals are excited, these points are located quasi-periodically; their number is apparently equal to the number of branches of the spiral. The spirals were excited, as a rule, in two stages. First, by adjusting the value of x_s, a caustic with a ring-

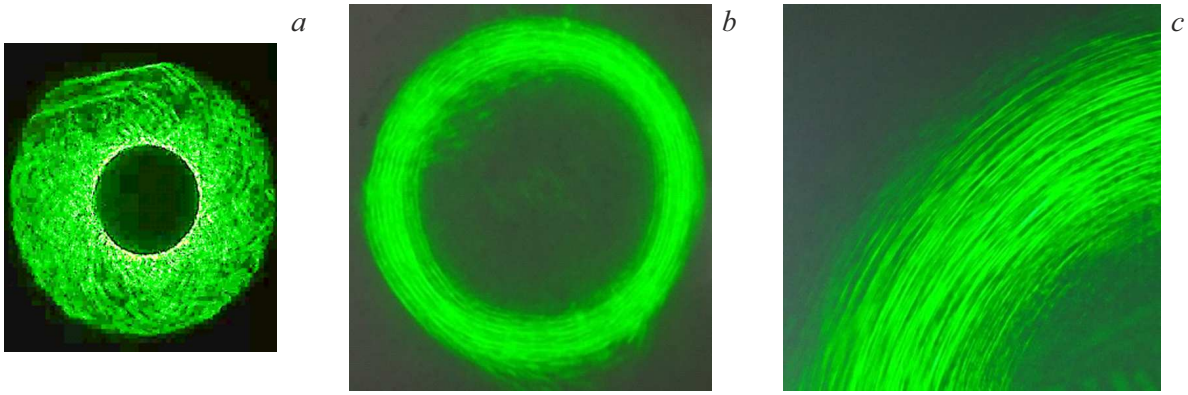

Figure 4. Radiation field intensity distributions ($\lambda = 532$ nm) for SP-SIEL/600 μm with a length of $l = 28$ cm in the near-field (a) and far-field (b/) regions; lens F 6.16-0.65. Photos were taken with $\delta \approx 1.5$ mm, $x_s \approx 100\,\mu$m, $\chi \approx 0.4$. Photo (c) shows a zoomed-in fragment of the image (b).

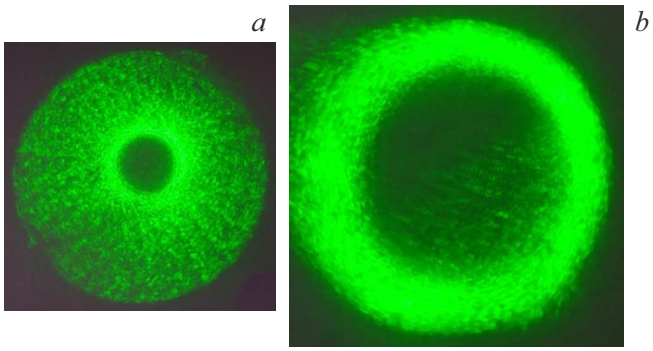

Figure 5. Radiation field intensity distributions ($\lambda = 532$ nm) for SP-SIEL/600 μm with a length of $l = 28$ cm in the near-field (a) and far-field (b) regions; lens F 6.16-0.65. Photos were taken with $\delta \approx 1.5$ mm, $x_s \approx 20\,\mu$m, $\chi \approx 0.18$.

Lens	LOMO 10×, 0.4	F-6.16A-0.65	F-2.8×, 1.25
δ_m, mm	6	2.5	1.8
d_{n}, μm	20.0	12.6	6.0
$\Delta\varphi$	1.7°	4.0°	11.3°
α_m	23.6°	40.5°	≈ 90°

envelope was obtained. Then, by fine-tuning the γ, Δ, y parameters, the ring-envelope was transformed into a spiral pattern.

It should be noted that the appearance of spiral structures in the far-field diffraction region (Fig. 3, *c, d*) presumably is indicative of the presence of optical vortices in the radiation emitted from the OF.

The ring-envelopes with a spotted pattern in the near-field region corresponded to caustics with a contrastless boundary. It has a relatively wide region of increased brightness (compared to the contrast region) and a lower contrast in the brightness of this region relative to the brightness on the periphery (Fig. 5, *a*). This is indicative of the excitation of a group of hybrid modes with a wider range of azimuthal numbers.

In terms of their topology, the radiation fields of SP-SIEL/200 μm, SP-SIEL/400 μm, and SP-SIEL/800 μm in the near-field and far-field regions are close to radiation fields of SP-SIEL/600 μm. In comparison with SP-SIEL/600 μm distributions, the first two OFs have a coarser pattern in the far-field region, the third OF has a finer pattern (Fig. 6). This can be explained by the fact that, at the same value of the nominal numerical aperture, the OF with a larger core diameter has a larger number of hybrid modes than the OF with a smaller core diameter. A larger number of excited hybrid modes results in a finer interference pattern.

Interference patterns formed by SP-SIEL/600 μm when using lenses with different numerical apertures

Fig. 7 shows photos of spiral distributions in the far-field region formed using lenses 10×, 0.4, F 6.16-0.65 and 2.8×, 1.25 (immersion). The caption to Fig. 7 shows values of the corresponding caustics χ.

It follows from the given data that the larger is the numerical aperture of the lens used, the more branches the formed spiral has and the smaller is the relative width of its ring-envelope. This is due to the difference in the diameters of the focused beam d_{n} and its angular divergence $\Delta\varphi$ for laser beams focused by the lenses used (Table 1).

A brief note should be made about the excitation of a silica-polymer OF with a Tefzel scattering reflective shell. Due to the strong scattering of light by the shell, especially the hybrid modes with large values of the azimuthal number m, we have failed to obtain a caustic with a contrast boundary in the SP-Tefzel/400 μm. Accordingly, spirals and

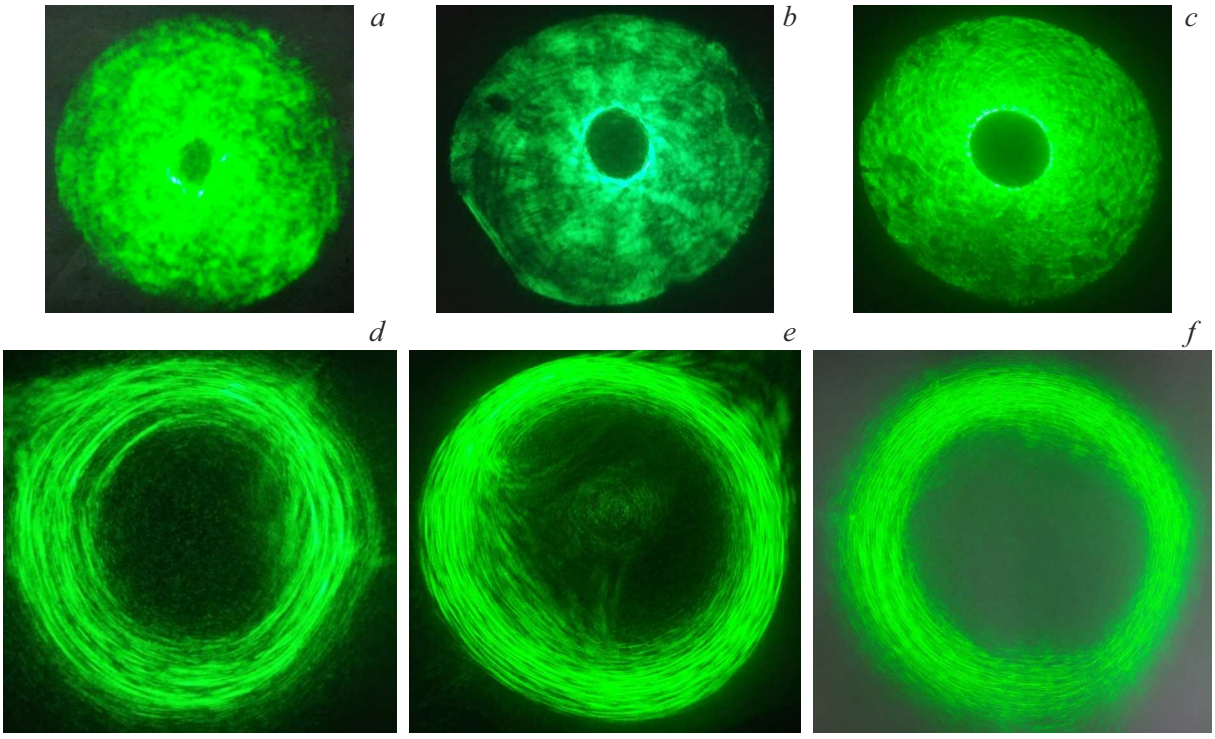

Figure 6. Radiation field intensity distributions ($\lambda = 532\,\text{nm}$) for SP-SIEL/200 μm with a length of $l = 40\,\text{cm}$ (a, d), SP-SIEL/400 μm with a length of $l = 15\,\text{cm}$ (b, e), and SP-SIEL/800 μm with a length of $l = 45\,\text{cm}$ (c, f); lens F 6.16-0.65. Photo (a, d) was taken with $\delta \approx 2\,\text{mm}$, $x_s \approx 20\,\mu\text{m}$, $\chi \approx 0.16$; photo (b, e) was taken with $\delta \approx 2\,\text{mm}$, $x_s \approx 80\,\mu\text{m}$, $\chi \approx 0.22$; photo (c, f) was taken with $\delta \approx 2\,\text{mm}$, $x_s \approx 200\,\mu\text{m}$, $\chi \approx 0.28$. The top photos were taken in the near-field region, the bottom photos were taken in the far-field region.

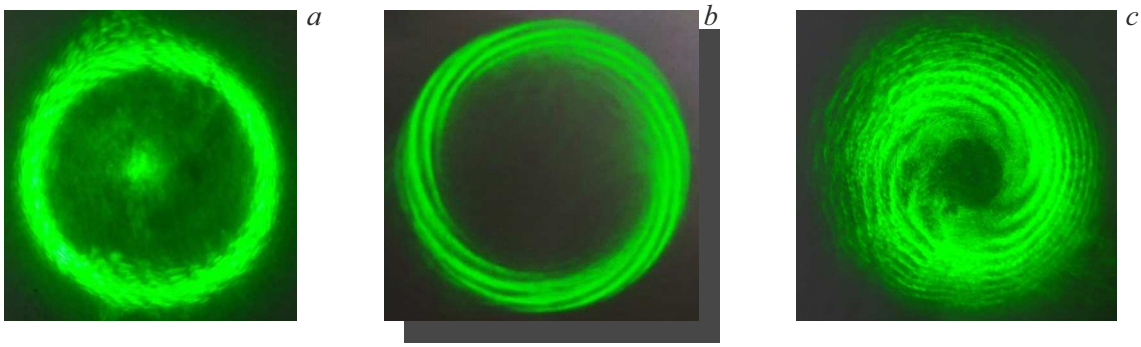

Figure 7. Radiation field intensity distributions ($\lambda = 532\,\text{nm}$) for SP-SIEL/600 μm with a length of $l = 20\,\text{cm}$ in the far-field region: (a) — lens $10^{\times}$, 0.4, δ4.5 m, $x_s \approx 20\,\mu\text{m}$, $\delta \approx 0.18$; (b) — lens F 6.16-0.65, $\delta \approx 1.8\text{mm}$, $x_s \approx 50\,\mu\text{m}$, $\chi \approx 0.22$; (c) — lens $2.8^{\times}$, 1.25, $\delta \approx 1.8\,\text{mm}$, $x_s \approx 140\,\mu\text{m}$, $\chi \approx 0.5$.

ring-envelopes with arc segments were not formed in the far-field region.

Conclusion

Experiments were carried out on the excitation of short ($10-50\,\text{cm}$) silica-polymer OFs with a core diameter of $200-800\,\mu\text{m}$ by laser radiation with $\lambda = 532\,\text{nm}$ using lenses with different numerical aperture values and under different excitation conditions. At the same time, the radiation intensity distributions were recorded in the near-field (at the output OF end) and in the far-field diffraction regions.

As a result of the experiments conducted, the interference pattern topologies in the far-field diffraction region typical for hybrid modes were identified: the bifilar spiral, the multifiral spirals, the ring-envelope with nested arc segments; the ring-envelope with filling similar to a blurred speckle pattern. Also, typical distributions of radiation intensity in the near-field diffraction region were identified: with contrast and contrastless caustics.

The spiral topologies recorded in the far-field diffraction region presumably are indicative of the presence of optical vortices in the radiation emitted from the OF. The most stable spiral patterns appeared in the SP-SIEL/600 μm optical fiber (with a nominal numerical aperture of NA = 0.44) when using a F 6.16-0.65 lens (with a numerical aperture of 0.65) and caustic values of $\chi = 0.12-0.22$. To more accurately identify optical vortices, an analysis of the phase characteristics of the radiation is required, which is the task of further studies.

Funding

This study has been carried out under the sate assignment of the Kotel'nikov Institute of Radio Engineering and Electronics of the RAS.

Conflict of interest

The authors declare that they have no conflict of interest.

References

[1] P.V. Korolenko, Sorosovskiy obrazovatelny zhurnal, № 6, 94 (1998) (in Russian).
[2] V.A. Soyfer, V.V. Kotlyar, S.N. Khonina, Fisika elementarnykh chastits i atomnogo yadra, **35** (6), (1368) (in Russian).
[3] S. Ramachandran, P. Kristensen. Nanophotonics, **2** (5-6), 455 (2013).
[4] D.V. Kizevetter, Kvant. elektron., **38** (2), 172 (2008) (in Russian).
[5] M.A. Bolshtyansky, A.Yu. Savchenko, B.Ya. Zel'dovich. Opt. Lett., **24** (7), 433 (1999).
[6] N.V. Ilyin, D.V. Kizevetter, Nauchno-Tekhicheskie Vedomosti SPbGPU, № 2, 9 (2010) (in Russian).
[7] V.I. Borisov, V.I. Lebedev, A.N. Kukanov, Pisma v ZhTF, **10** (5), 287 (1984) (in Russian).
[8] A.V. Volyar, T.A. Fadeeva, Pisma v ZhTF, **22** (8), 54 (1996) (in Russian).
[9] D.V. Kizevetter, Optichesky Zhurnal, **74** (9), 20 (2007) (in Russian).
[10] D.V. Kizevetter, N.V. Ilyin, Nauchno-Tekhicheskie Vedomosti SPbGPU, № 3 (177), 151 (2013) (in Russian).
[11] A.A. Makovetsky, Opt. i spektr., **129** (6), 1198 (2021) (in Russian).

Translated by Y.Alekseev